Veterinary Microbiology 234 (2019) 8–16

Contents lists available at ScienceDirect

Veterinary Microbiology

journal homepage: www.elsevier.com/locate/vetmic

A combined metabolomic and bioinformatic approach to investigate the function of transport proteins of the important pathogen *Mycoplasma bovis*

Yumiko Masukagami[a], Brunda Nijagal[b], Sara Mahdizadeh[a], Chi-Wen Tseng[a], Saravanan Dayalan[b], Kelly A. Tivendale[a], Philip F. Markham[a], Glenn F. Browning[a,1], Fiona M. Sansom[a,1,*]

[a] Asia-Pacific Centre for Animal Health, Melbourne Veterinary School, Faculty of Veterinary and Agricultural Sciences, The University of Melbourne, Victoria, Australia
[b] Metabolomics Australia, The Bio21 Institute of Molecular Science and Biotechnology, The University of Melbourne, Parkville, Victoria, Australia

ARTICLE INFO

Keywords:
Mycoplasma bovis
Metabolomics
Transport proteins

ABSTRACT

Mycoplasma bovis is an economically important pathogen of the cattle industry worldwide, and there is an urgent need for a more effective vaccine to control the diseases caused by this organism. Although the *M. bovis* genome sequence is available, very few gene functions of *M. bovis* have been experimentally determined, and a better understanding of the genes involved in pathogenesis are required for vaccine development. In this study, we compared the metabolite profiles of wild type *M. bovis* to a number of strains that each contained a transposon insertion into a putative transporter gene. Transport systems are thought to play an important role in survival of mycoplasmas, as they rely on the host for many nutrients. We also performed ^{13}C-stable isotope labelling on strains with transposon insertions into putative glycerol transporters. Integration of metabolomic and bioinformatic analyses revealed unexpected results (when compared to genome annotation) for two mutants, with a putative amino acid transporter (MBOVPG45_0533) appearing more likely to transport nucleotide sugars, and a second mutant, a putative dicarboxylate/amino acid:cation (Na^+ or H^+) symporter (DAACS), more likely to function as a biopterin/folate transporter. This study also highlighted the apparent redundancy in some transport and metabolic pathways, such as the glycerol transport systems, even in an organism with a reduced genome. Overall, this study highlights the value of metabolomics for revealing the likely function of a number of transporters of *M. bovis*.

1. Introduction

Mycoplasma bovis is an important pathogen of cattle worldwide, causing a variety of significant diseases, including bovine respiratory disease, an economically important disease in feedlots (Rosengarten and Citti, 1999). In addition, *M. bovis* causes mastitis, arthritis and otitis media (Caswell and Archambault, 2007; Caswell et al., 2010; Nicholas and Ayling, 2003; Rodriguez et al., 1996). Current control methods for *M. bovis* are limited, as the few vaccines available are of questionable efficacy (Caswell and Archambault, 2007; Nicholas et al., 2007) and antimicrobials do not appear to be effective in eliminating chronic infection (Ayling et al., 2000; Nicholas and Ayling, 2003; Pfutzner and Sachse, 1996). In order to develop effective vaccines, it is crucial to develop a better understanding of the pathogenesis of *M. bovis*. Like all mycoplasmas, *M. bovis* has undergone genome reduction and relies on the host for many of its metabolic requirements in order to survive and therefore cause disease (Caswell and Archambault, 2007; Halbedel and Stulke, 2007; Minion, 2002; Razin et al., 1998; Sharma et al., 2014; Tozzi et al., 2006; Voelker and Dybvig, 1996). It is particularly important for mycoplasmas to scavenge exogenous nutrients from the extracellular milieu in order to support themselves, as they lack many of the genes required for biosynthesis (Fraser et al., 1995; Razin, 1969).

Transport systems in bacteria play a crucial role in the uptake of a broad range of nutrients, as well as in the efflux of waste products and drugs, and the transport of components such as polysaccharides and peptides to the cell surface (Bachmann, 1990; Davidson and Chen, 2004; Lee, 2009). In this study, two different metabolomic approaches were utilised to help elucidate the function of several putative transporters of *M. bovis*. Several mutants, each containing a transposon insertion in a gene encoding a putative transporter or component of a transport system, were analysed using LC/MS and their metabolite profiles compared to that of the wild type *M. bovis* strain. Secondly,

* Corresponding author.
E-mail address: fsansom@unimelb.edu.au (F.M. Sansom).
[1] These authors contributed equally.

https://doi.org/10.1016/j.vetmic.2019.05.008
Received 27 November 2018; Received in revised form 3 May 2019; Accepted 7 May 2019

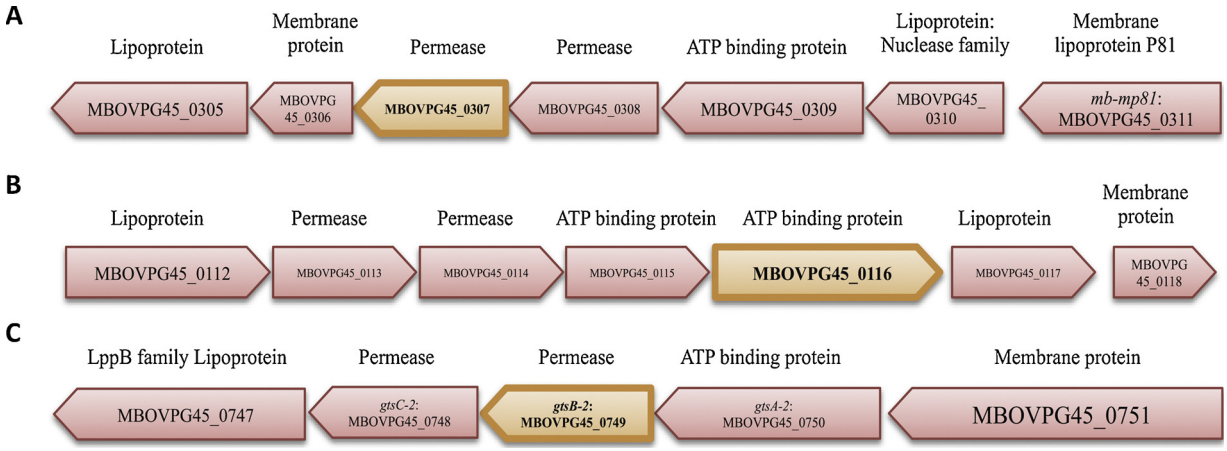

Fig. 1. ABC transporter operons disrupted in this study. (A) ABC transporter operon containing MBOVPG45_0307. (B) ABC transporter operon containing MBOVPG45_0116. (C) ABC transporter operon containing MBOVPG45_0749. The arrow outline in bold indicates the genes that have been disrupted by transposon insertion. Putative functions of the encoded proteins, based on genome annotations and bioinformatic analysis, are listed above each gene.

targeted GC/MS analysis combined with ^{13}C-glycerol labelling was used to further investigate the function of putative glycerol transporters.

Mutant ΔMBOVPG45_0307 contains an insertion in MBOVPG45_0307, a gene encoding a putative nucleotide binding protein that lies within a predicted ABC transporter operon (MBOVPG45_0305 to MBOVPG45_0310) (Fig. 1A) (Sharma et al., 2014).

A second mutant contained an insertion in MBOVPG45_0116, which is annotated as an ABC transporter ATP-binding protein (Fig. 1B). Two more mutants, MBOVPG45_0533, which encodes a putative L-type amino acid transporter (LAT), and MBOVPG45_0568, which encodes a putative dicarboxylate/amino acid:cation (Na^+ or H^+) symporter (DAACS) responsible for the uptake of certain amino acids (Saier, 2000), were selected. All these mutants were profiled using LC/MS.

Two additional mutants contained insertions in potential glycerol transporter genes. MBOVPG45_0530, annotated as the glycerol uptake facilitator gene *glp*F, which encodes a transmembrane solute transporter that, in other bacterial species, has been shown to transport glycerol across the bacterial cell membrane (Saier, 2000; Truniger and Boos, 1993), and MBOVPG45_0749, annotated as the glycerol permease gene *gts*B in the glycerol ABC transporter operon (Fig. 1C), were analysed using targeted metabolomics employing ^{13}C-glycerol labelling and GC/MS analyses.

2. Materials and methods

2.1. Mycoplasma strains and culture

To compare the metabolite profiles of wild type *M. bovis* PG45 and selected *M. bovis* transposon mutants (Table S1), bacteria were grown in air at 37 °C in modified Frey's broth, referred to here as *M. bovis* (MB) medium (0.21% Difco PPLO base (Becton Dickinson), 0.56% yeast extract, 10% inactivated swine serum, 0.0064% phenol red solution, penicillin G at 0.3 mg ml^{-1}, pH adjusted to 7.8) (Sharma et al., 2014). Gentamicin (50 µg ml^{-1}) was added to the medium to maintain selective pressure for the presence of the transposon in the *M. bovis* mutants. Strains were passaged routinely by dilution at 1:10 in fresh medium, followed by 24 h of incubation. For metabolite extraction, mycoplasma cells were passaged twice, and on the third passage cells were diluted 1:10 and 8 × 20 ml biological replicates were incubated in 50 ml conical centrifuge tubes (Fisher Scientific) for 18 h for wild type *M. bovis* PG45 and most mutant strains (ΔMBOVPG45_0307, ΔMBOVPG45_0116, ΔMBOVPG45_0530, ΔMBOVPG45_0568 and ΔMBOVPG45_749), with the exception of ΔMBOVPG45_533, which was incubated for 24 h, due to slower growth rate of this mutant.

2.2. Screening PCR and sequence analysis for M. bovis transposon mutants

Previous work used transposon mutagenesis to generate libraries of *M. bovis* mutants in which genes were disrupted by the insertion of a Tn*4001* transposon (Sharma et al., 2014). PCR analysis was conducted to confirm the presence and position of the transposon using specific primers designed to detect the position of the transposon within the gene of interest (GOI) (Sharma et al., 2014) (Table S1). The IR inverse primer was used to detect the end of the transposon sequence in *M. bovis* mutants, and was paired with specific primers for the GOI (Table S1). PCR reactions were performed using GoTaq DNA polymerase (Promega) according to the manufacturer's instructions. Briefly, 20 µl reactions (containing 200 ng template mycoplasma genomic DNA, 1 × green reaction buffer, 1 µM of the forward and of the reverse primer, 200 µM of each dNTP and 1.5 U of GoTaq DNA polymerase (Promega)) were incubated in an iCycler thermocycler (Bio-Rad). The cycling conditions consisted of an initial denaturing step (94 °C for 5 min), followed by 28 cycles of denaturing (94 °C, 30 s), annealing (52 °C, 30 s) and extension (72 °C, 45 s), and then a final extension step at 72 °C for 5 min. The PCR products were separated by 1.5% agarose gel electrophoresis at 10 V cm^{-1}. The PCR products were sequenced to confirm insertion of the transposon into the GOI, with BLAST and the National Centre for Biotechnology Information (NCBI) nucleotide sequence database (https://www.ncbi.nlm.nih.gov) used to confirm the identity of the GOI in *M. bovis* PG45 (Wise et al., 2011).

2.3. Measurement of viable numbers of M. bovis using titration assays

Transposon mutants were revived from stocks stored at −80 °C by 1:10 dilution in fresh MB medium and incubation at 37 °C for 18 h. Growth was measured from the exponential to the stationary phase for wild type *M. bovis* PG45 (16 to 32 h) and the mutants (18 to 30 h), with ΔMBOVPG45_0307 measured in triplicate, and ΔMBOVPG45_0116, ΔMBOVPG45_0530, ΔMBOVPG45_0533, ΔMBOVPG45_0568 and ΔMBOVPG45_0749 in duplicate (Table 1, Fig. S1). Each replicate consisted of a 10 ml culture, prepared by 1:10 dilution of a stationary phase culture, with 240 µl samples were taken at selected time points. At each time point, titration by limiting dilution in MB broth in 96 well plates (Thermo Fisher Scientific) was used to determine the number of viable mycoplasmas in the cultures, with bacterial growth detected by the observation of a change in the colour of the medium, as described previously (Stemke and Robertson, 1982). Briefly, 25 µl of culture was dispensed into each well of the first column of a 96 well plate containing 225 µl of MB medium per well. The cultures in the first column were then serially diluted 10-fold until column 10 was reached, with

Table 1
Mycoplasma viable cell numbers between 16 and 32 h.

Strains	Incubation time (h)	CCU ml^{-1}
M. bovis PG45	16	2.35×10^8
	24	1.32×10^9
	32	2.58×10^8
ΔMBOVPG45_0307	18	2.76×10^8
	24	5.26×10^8
	30	6.28×10^8
ΔMBOVPG45_0116	18	8.99×10^8
	24	7.13×10^8
	30	1.75×10^9
ΔMBOVPG45_0530	18	4.21×10^8
	24	9.88×10^8
	30	1.05×10^9
ΔMBOVPG45_0533	18	4.16×10^8
	24	9.97×10^8
	30	1.96×10^9
ΔMBOVPG45_0568	18	1.39×10^9
	24	7.33×10^8
	30	1.17×10^9
ΔMBOVPG45_0749	18	1.95×10^9
	24	2.00×10^9
	30	1.55×10^9

columns 11 and 12, containing only sterile broth, used as uninoculated controls. Plates were incubated for 3 weeks, then the number of wells in the last 3 columns showing a colour change were counted, and this used to determine the most probable number (MPN) of mycoplasmas present in the original inoculum using an online MPN calculator (version 3, (http://www.i2workout.com/mcuriale/mpn/)) for Windows.

2.4. Metabolic quenching and extraction of polar metabolites

Late logarithmic phase cultures (as determined by the growth curves) were rapidly quenched to 0 °C in an ethanol/dry ice bath to halt metabolic activity. After quenching, mycoplasma cells were harvested by centrifugation (20,000*g*, 20 min, 0 °C) and the cell pellets re-suspended in ice-cold phosphate buffered saline (PBS). Cell numbers were adjusted to 1×10^{10} CCU (based on the growth curves for identical strains cultured under similar conditions), then the cell pellets were washed twice with PBS (17,100*g*, 5 min, 0 °C) to remove residual culture medium, and then extracted using chloroform:methanol:water ($CHCl_3$:CH_3OH:H_2O, 1:3:1 v/v/v, 250 µl) containing 1 nmol ^{13}C-sorbitol and 10 nmol $^{13}C_6$-^{15}N-valine as internal standards. After vigorous vortex mixing, the samples were incubated at 60 °C for 15 min to lyse the bacterial cells. Cell debris was removed by centrifugation (17,100*g*, 5 min, 0 °C) and the supernatant adjusted to $CHCl_3$:CH_3OH:H_2O (1:3:3 v/v/v) by addition of dH_2O, before vigorous mixing and centrifugation (17,100*g*, 5 min, 0 °C) to induce phase separation. The upper aqueous phase, containing polar metabolites, was transferred to a fresh pre-cooled 1.5 ml microfuge tube and stored at −80 °C until LC/MS analysis.

2.5. LC/MS analysis of polar metabolites

Polar metabolites were analysed by high performance (HP) LC/MS as described previously (Masukagami et al., 2018). Analysis was performed on an Agilent 1200 series HPLC system (Agilent Technologies). Samples were stored in an autosampler at 4 °C. Metabolite separation was performed by injecting a 10 µl sample onto a SeQuant ZIC-pHILIC column (150 mm × 4.6 mm, 5 µm) maintained at 30 °C using Solvent A (20 mM $(NH_4)_2CO_3$, pH 9.0 (Sigma-Aldrich) and Solvent B (100% acetonitrile) at a flow rate of 300 µl.min^{-1}.

The gradients used were: time (t) = 0 min, 80% B; t = 0.5 min, 80% B; t = 15.5 min, 50% B; t = 17.5 min, 30% B; t = 18.5 min, 5% B, t = 21.0 min, 5% B; t = 23 min, 80% B. The mass spectrometry analysis was performed on an Agilent 6545 series quadrupole time-of-flight mass spectrometer (QTOF MS) (Agilent Technologies). The LC flow was directed to an electrospray ionisation source (ESI), where metabolite ionisation in negative mode was performed with a capillary voltage of 2500 V, a drying gas (N_2) pressure of 20 psi with a gas flow rate of 10.0 L.min^{-1}, a gas temperature in the capillary of 325 °C and fragmentor and skimmer cap voltages of 125 V and 45 V, respectively. LC/MS data was collected in centroid mode with a scan range of 60–1200 m/z and an acquisition rate of 1.5 spectra sec^{-1} in all-ion fragmentor (AIF) mode, which included three collision energies (0, 10, 20 V).

Prior to analysis, mass calibration was performed for negative mode to 0.5 ppm accuracy of the m/z value. Internal mass calibration was performed using Agilent ESI-TOF Reference Mass Solution containing purine (119.036320) and hexakis (1H,1H,3H-tetrafluoropropoxy) phosphazine (981.99509) (API-TOF Reference Mass Solution Kit, Agilent technologies), which was continuously infused into the ESI source at a flow rate of 200 µl.min^{-1}.

2.6. Identification of metabolites

Targeted data matrices were generated using MassHunter Quantitative Analysis software (version B.07.00, Agilent Technologies) with metabolite identification (Metabolomics Standard Initiative (MSI) level 1) based on the retention time and molecular masses matching (with an error < 10 ppm allowable) to an authentic standards in the in-house Metabolomics Australia library (authentic standards) (Sumner et al., 2007).

Profiles obtained from LC/MS analysis were filtered to remove the noise peaks above the specific abundance threshold. Metabolites were identified by comparison of retention time and molecular mass, with an error < 10 ppm allowable when comparing to the mass accuracy of the compounds in the in-house library. Peak integration was performed on the spectra from identified metabolites with the in-house library, and collated into a targeted data matrix.

2.7. Statistical analysis and comparison of metabolite profiles of M. bovis PG45 and M. bovis transposon mutants

The statistical analyses were conducted on LC/MS targeted data matrices as described previously (Masukagami et al., 2018). Prior to statistical analyses, median normalisation was performed on the data matrices, with every metabolite's peak abundance value divided by the median value of all the metabolites of an individual sample. This accounted for any difference in cell number between samples, as it brought all the metabolites and their observed peak values from differing samples to the same base level, and thus enabled meaningful statistical comparisons to be performed even if the exact cell number of each sample varied.

2.8. Labelling studies with ^{13}C-glycerol

Labelling studies were conducted with ^{13}C-glycerol, with targeted detection of the incorporation of ^{13}C-label into the intracellular glycerol and related metabolite pool. Cultures were passaged as described above, before labelling for 18 h for wild type *M. bovis* PG45 and ΔMBOVPG45_0749, and 24 h for ΔMBOVPG45_0530 (to account for differences in growth rates), in standard MB medium containing an additional 1 mM ^{13}C-glycerol. Cultures were then quenched, polar metabolites extracted with 1 nmol scyllo-inositol as an internal standard, and the extracts analysed by GC/MS.

The labelled metabolite spectra were subtracted from those containing the naturally occurring isotope of carbon, then all metabolites were corrected for background labelling based on a protocol and principles described previously (Kowalski et al., 2015). The level of labelling of each metabolite was recorded as a proportion of the total,

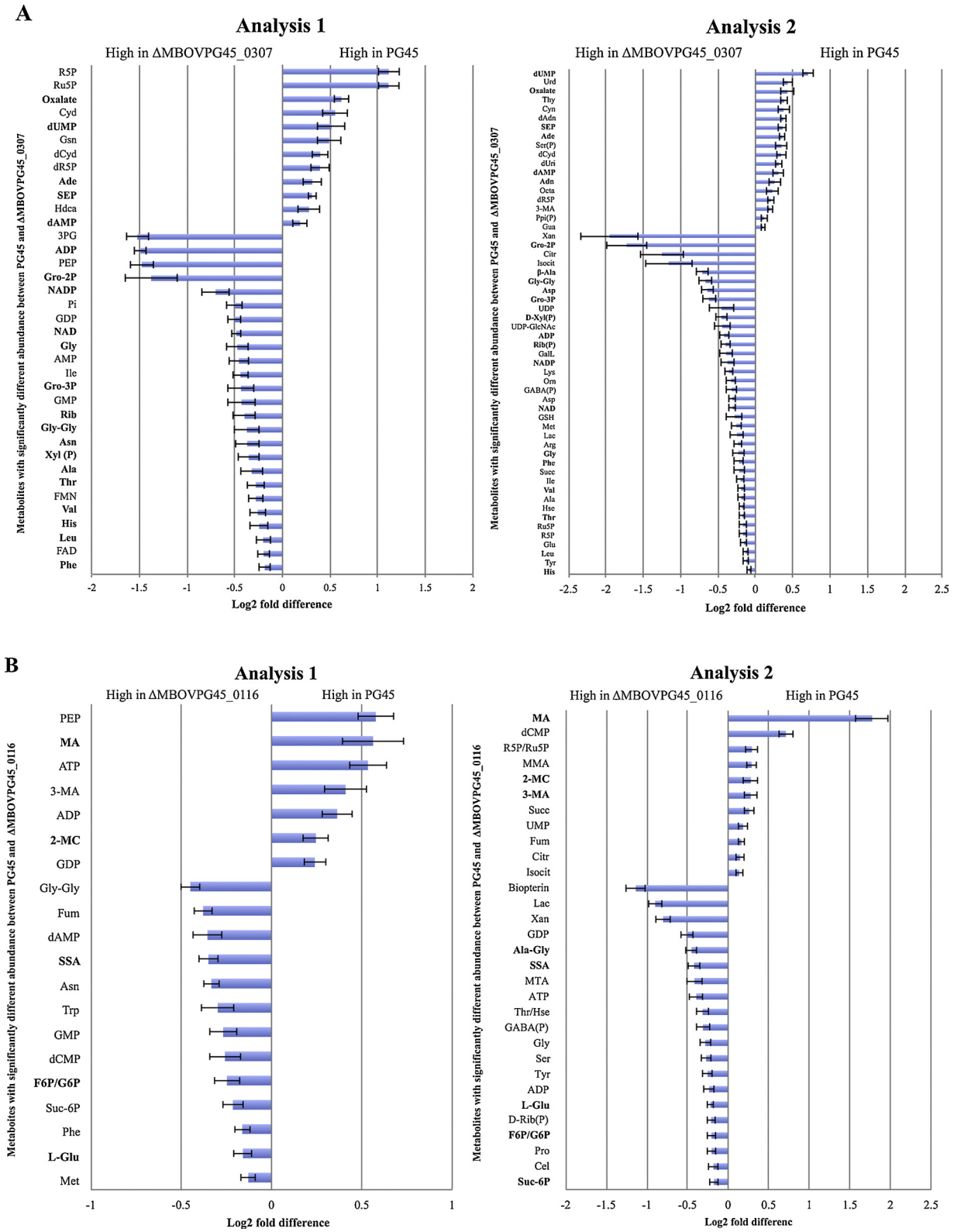

Fig. 2. Relative abundances of metabolites in (A) ΔMBOVPG45_0307, (B) ΔMBOVPG45_0116, (C) ΔMBOVPG45_0533 and (D) ΔMBOVPG45_0568, compared to wild type *M. bovis* PG45. Only significantly different ($P < 0.05$, unpaired BH-adjusted Student's *t*-test) metabolites are shown. Results depict two independent LC/MS analyses (each containing 8 biological replicates). Metabolites in bold text were consistently different across both independent LC/MS analyses. Metabolites marked with a suffix (P) were identified putatively by comparison with authenticated in-house standards. Abbreviations for metabolites are defined in Table S2.

and these data were used to create a bar graph in EXCEL and a heat map using an R script, as previously described (Saunders et al., 2014). An unpaired Student's *t*-test was used to compare the proportions of label detected in the wild type and each individual mutant in the total intracellular glycerol pool.

2.9. Metabolite derivatisation and GC/MS analysis

The ^{13}C-glycerol labelled samples were transferred into glass vial inserts and completely dried in a rotational vacuum concentrator (John Morris Scientific RVC-2-33) at 37 °C, with 30 µl of 100% methanol added for the final drying stage. Free aldehyde groups were protected by derivatisation in methoxyamine chloride (Sigma, 20 µl, 30 mg ml^{-1} in pyridine) with continuous mixing (2 h, 37 °C). Metabolites were then derivatised by treatment with 20 µl of N, O-bistrimethylsilyltrifluoroacetamide (BSTFA) containing 1% trimethylchlorosilane (TMCS) (Thermo Scientific) (1 h, 37 °C, continuous shaking) using a Gerstel MPS2 autosampler robot. For GC/MS analysis, 1 µl of derivatised sample was injected into an Agilent 7890A gas chromatograph (split/splitless inlet, 250 °C) containing a VF-5 ms column (30 m, 250 µm, 0.25 µm + 10 m Eziguard precolumn) coupled to an Agilent 5975C mass selective detector. Helium was used as the carrier gas at a constant flow rate of 1 ml.min^{-1}. The GC temperature was ramped from 35 °C, at which it was initially held for 2 min, to 325 °C, at a rate of 25 °C.min^{-1}, and then held for 5 min at 325 °C. A 5975 mass selective detector was used in scan mode and mass spectra data were collected at 9.19 scans/s over an m/z range of 50–600.

2.10. Bioinformatics and database searches for protein function

The similarity of the putative *M. bovis* proteins to other proteins was determined by searching the NCBI (using BLASTP (Altschul et al., 1997)) and/or BioCyc (Caspi et al., 2016; Karp et al., 2005) databases. Sequences used for searching were the translated nucleotide sequences obtained from the *M. bovis* PG45 genome sequence. The protein structure prediction tools I-TASSER (Roy et al., 2010) and Phyre^2 (Kelley et al., 2015) were also used to assist in prediction of protein function. When conducting Phyre^2 analysis, the alignment confidence represents the probability that the observed alignment between the two protein sequences represents true homology (Kelley et al., 2015). Confidence levels above 90% are considered to indicate high accuracy (Kelley et al., 2015). The alignment confidence is combined with the percentage of identity between the query sequence and the template to predict the overall accuracy (Kelley et al., 2015). An identity of greater than 30% is considered to have extremely high accuracy, but even with a sequence identity of less than 15% the model can be very useful as long as the confidence is high (Kelley et al., 2015).

3. Results

3.1. Metabolite profiling and bioinformatic analysis suggests that the MBOVPG45_0307 protein is part of a nucleotide ABC transporter

The predicted nucleotide binding function of *MBOVPG45_0307* was based on the genomic context (Fig. 1A), which includes a putative nuclease family gene (MBOVPG45_0310), as well as the *M. bovis* membrane protein 81 gene (*mb-mp81*) (MBOPVG45_0311), a homologue of an *M. gallisepticum* nucleotide binding protein (Masukagami et al., 2013), adjacent to the ABC transporter genes (Fig. 1A). This operon is also annotated as an oligosaccharide ABC transporter in the Genbank (Altschul et al., 1990, 1997) and BioCyc (Caspi et al., 2016; Karp et al., 2005) databases. A total of 73 and 113 metabolites were identified in the metabolite profiles of wild type *M. bovis* PG45 and the ΔMBOVPG45_0307 mutant, respectively, in two independent LC/MS analyses (each analysis contained 8 biological replicates per strain). Although the fold differences in abundance were relatively small, 5 metabolites were significantly more abundant in wild type *M. bovis* PG45 and 16 metabolites were more abundant in ΔMBOVPG45_0307 across both independent analyses (Fig. 2A). Metabolites related to nucleotide metabolic pathways, namely dUMP, dAMP, deoxycytidine (dCyd) and adenine, were more abundant in the wild type, whereas ADP, NAD and NADP were more abundant in ΔMBOVPG45_0307 (Fig. 2A). Ribose (Rib), xylose (Xyl), glycerol-2-phosphate (Gro-2 P) and sn-glycerol-3-phosphate (Gro-3 P) were also consistently higher in ΔMBOVPG45_0307 (Fig. 2A).

The amino acid sequence of the MBOVPG45_0307 protein was further analysed using the Phyre^2 tool. Phyre^2 predicted that MBOVPG45_0307 contained a MetI domain, with an alignment confidence of 100% and 19% identity with other proteins. The MetI superfamily contains methionine and maltose uptake permeases. Six transmembrane helices were predicted, with a signal peptide of 1–38 amino acids at the N-terminal end of the protein and both the N and C termini exposed to the extracellular environment. Alignment with a DNA/RNA binding 3-helical bundle (Accession number 1umq A in SCORPe (Fox et al., 2014)) and a DNA binding protein from *Rhodobacter sphaeroides* (Accession number 1UMQ in RCSB PDB (www.rcsb.org)) (Berman et al., 2000; Laguri et al., 2003) was also predicted for the MBOVPG45_0307 amino acid sequence at residues 200–230, although the accuracy of this model was low, with an alignment confidence of approximately 10–13% and an identity of 10–13%. Overall, although Phyre^2 analysis revealed greater similarity to maltose permeases and sugar binding domains than to nucleotide binding proteins, no sugars were significantly elevated in abundance in wild type in either analysis. Therefore, when combined with the metabolite profiling results, the overall analysis suggested that the MBOVPG45_0307 protein may bind nucleotides, as part of an ABC-transporter that transports nucleotides, which is at odds with the current annotation of this transporter as an oligosaccharide transporter. Future work using stable isotope labelled compounds would be useful to definitively elucidate the function of this transporter.

3.2. Bioinformatic analysis suggests that the MBOVPG45_0116 protein is an NBD protein within an ABC transporter, but metabolite profiling did not identify a likely substrate

A total of 109 and 107 metabolites were identified using the authenticated in-house standards library in the metabolite comparisons between wild type *M. bovis* PG45 and the ΔMBOVPG45_0116 mutant across two independent LC/MS analyses. Again, the observed significant differences in identified metabolites were small, with the $\log_2$ fold difference ranging from 0.12 to 1.77 (Fig. 2B). Maleic acid (MA) was consistently significantly more abundant in *M. bovis* PG45 than in ΔMBOVPG45_0116, with fold differences of 0.5 and 1.8 (Fig. 2B), as were 3-methyladenine (3-MA) and 2-methylcitrate (2-MC). The Phyre^2 analysis predicted MBOVPG45_0116 to be an ATP-binding protein within an ABC transporter, as crystal structures of several ATP-binding proteins from different putative ABC transporters corresponded with the protein structure of MBOVPG45_0116, with an alignment confidence of 100% and 30% to 50% identity. The substrates of the similar transporters varied widely and included sugars, amino acids, dipeptides, oligopeptides and nickel, which is to be expected, as the structure of ATP-binding proteins is highly conserved within ABC transporters. Unfortunately, metabolite profiling did not suggest a likely substrate for this *M. bovis* transporter, as none of the metabolites that were higher in the wild type were key compounds in *M. bovis* metabolism, and nor were they likely to be transported by this class of transporter.

3.3. Metabolite and bioinformatic analyses suggest that MBOVPG45_0533 is involved in nucleotide sugar transport

The putative protein encoded by MBOVPG45_0533 is annotated as an L-type amino acid transporter, which is further classified within the

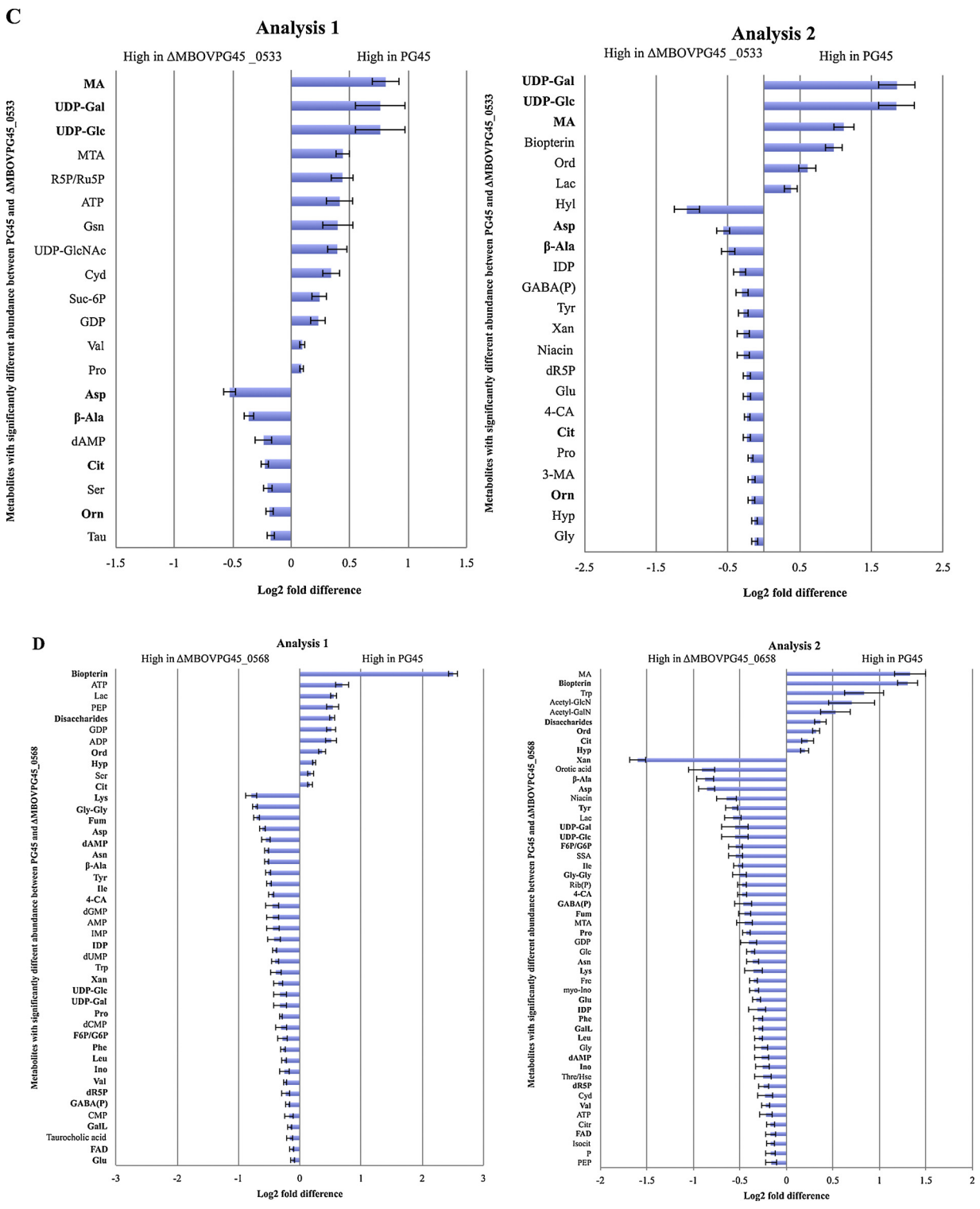

Fig. 2. (*continued*)

amino acid-polyamine-organocation (APC) superfamily for the uptake of neutral amino acids (Saier, 2000), In the metabolite profiling experiments, a total of 109 and 107 metabolites were identified using the authenticated in-house standards library for both wild type *M. bovis* PG45 and the ΔMBOVPG45_0533 mutant across the two independent LC/MS analyses. Of these metabolites, the UDP-sugars, UDP-D-galactose and UDP-glucose, and maleic acid (MA) were consistently more abundant in *M. bovis* PG45 than in ΔMBOVPG45_0533, with fold differences of 0.7 to 1.8 (Fig. 2C). Phyre^2 analysis predicted thirteen transmembrane domains, a cytoplasmic N-terminus and an extracellular C-terminus within the putative MBOVPG45_0533 protein. This analysis also revealed similarity with both a nucleoside-cation-symport-1 family 2 transporter (accession number 2JLN in RCSB PDB) (Berman et al., 2000; Weyand et al., 2008) and a sodium/glucose co-transporter (accession number 3DH4 in RCSB PDB) from *Vibrio parahaemolyticus* (Faham et al., 2008), with alignment confidences of 99.9% and 98.3%, respectively, and sequence identities of 11% with both. Taken together, these results suggest that MBOVPG45_0533 imports nucleotide sugars,

as these were more abundant in the wild type cells.

No significant differences in neutral amino acid abundances were observed, but L-aspartic acid (Asp), β-alanine (β-Ala), citrulline (Cit) and ornithine (Orn) were significantly more abundant in the MBOVPG45_0533 mutant, although with very small fold differences (Fig. 2C). Phyre[2] analysis also revealed similarity with an antiporter for glutamate and γ-aminobutyric acid (GABA), with an alignment confidence of 100% and an identity of 13%. This antiporter is closely related to the LAT transporter family, within the broader APC transporter superfamily. This similarity may suggest that MBOVPG45_0533 transports amino acids, but when combined with the observed changes in metabolite levels, it appears likely that MBOVPG45_0533 would only be exporting amino acids. In both analyses, the fold difference for the nucleotide sugars were greater than the changes in amino acids.

3.4. Analysis of the putative DAACS family transporter protein (MBOVPG45_0568) mutant suggests it may transport biopterin

A total of 109 and 107 metabolites were identified using the authenticated in-house standards library in the metabolite comparisons of wild type *M. bovis* PG45 and the ΔMBOVPG45_0568 mutant across the two independent LC/MS analyses. The $\log_2$ fold differences were again small, ranging from 0.12 to 2.5 (Fig. 2D). Of those metabolites that were significantly different across both analyses, the highest fold differences were for biopterin (1.3 and 2.5), which was significantly more abundant in wild type *M. bovis* PG45 in both independent analyses (Fig. 2D). No other metabolites differed significantly in abundance between the two strains by a log fold difference of more than one across both analyses.

Eleven transmembrane helices were predicted within the amino acid sequence of MBOVPG45_0568. Phyre[2] predicted similarity to a glutamate transporter from *Thermococcus kodakarensis* (accession number 4KY0 in RCSB PDB) (Berman et al., 2000), with an alignment confidence of 100% and 25% identity. Residues 15–135 also had low similarity to the substrate-specific component (S-component) of a thiamine binding protein within an ABC transporter (Accession number 2RLB in RCSB PDB) (Erkens et al., 2011), although the alignment confidence was only 35.5% and the identity 15%. Folate and biopterin are related to thiamine, and the similarity of their chemical structures is shown in Fig. 3. Together, these results suggest that biopterin may be transported by MBOVPG45_0568.

3.5. Incorporation of ^{13}C-glycerol into M. bovis PG45 and the MBOVPG45_0530 and MBOVPG45_0749 glycerol transporter mutants

To examine the impact of transposon insertion into either of the putative glycerol transporter genes, ^{13}C-glycerol uptake was compared between wild type and the two glycerol transporter gene mutants (ΔMBOVPG45_0530 and ΔMBOVPG45_0749). No significant differences were detected in the proportions of the ^{13}C-label incorporated into intracellular glycerol, indicating no significant difference in uptake (Fig. 4A). Furthermore, a medium analysis investigating depletion of nutrients at 0, 5, 30, 60, 270 and 480 min detected no significant differences between the strains in medium components at any time point. However, surprisingly, the incorporation of ^{13}C-label into the glycerol pool was 6–8%, while the glycerol 3-phosphate (Gro-3 P) pool incorporated 15–20% of the label in both wild type *M. bovis* PG45 and the two mutants (Fig. 4B), suggesting dilution of the intracellular glycerol pool from another (unlabelled) source.

4. Discussion

The small $\log_2$ fold differences observed throughout this study may reflect alternative transporters or metabolic pathways that complement the missing function(s) of the genes interrupted by the transposon. This may suggest that, despite the genome reduction seen in mycoplasmas, there is still significant redundancy within metabolic pathways. Nevertheless, metabolites that differed significantly in abundance across both analyses, each of which contained 8 biological replicates, despite the small fold differences, may actually reflect the true function of the protein under study.

The metabolite and bioinformatic analyses suggested that MBOVPG45_0307 is likely to play a role in the uptake of nucleotides and nucleotide precursors into the cell, with greater abundance of dUMP, dAMP, deoxycytidine and adenine in the wild type compared to the transposon mutant. However, the small magnitude of the differences suggests that any deficiency in nucleotide precursor uptake is compensated for by other nucleotide transporters. A substrate-binding ATP-dependent ABC transport system (UptBACD) involved in the uptake of nucleosides was described in *M. bovis* strain M23 (Lee, 2009), in which *uptB*, encoding the substrate binding protein, and *uptA*, encoding the ATP-binding protein, are homologous to MBOVPG45_0016 and MBOVPG45_0018, respectively, so this UptBACD transporter may be one of the compensatory transporters. However, accumulation of the putatively identified pentose sugars ribose and xylose was also seen in ΔMBOVPG45_0307, which could reflect another compensatory pathway for dysfunctional nucleotide uptake in the MBOVPG45_0307 mutant. These two pentose sugars could be incorporated into the pentose phosphate pathway to supply 5-phosphoribosyl diphosphate (PRPP) for nucleotide synthesis, and the higher abundance in the mutant could suggest that synthesis or uptake of these sugars is increased in the mutant as the demand for them is increased. Stable carbon isotope labelling with, for example, ^{13}C-glucose to compare flux through the pentose phosphate pathway in the wild type and ΔMBOVPG45_0307 would be useful in investigating these results further. Although the conserved domain of this protein is annotated as a Gro-3 P ABC transporter permease in the NCBI database, Gro-2 P and Gro-3 P were consistently elevated in the ΔMBOVPG45_0307 metabolome, suggesting that this transporter is not responsible for uptake of Gro-3 P, consistent with our results suggesting that it actually transports

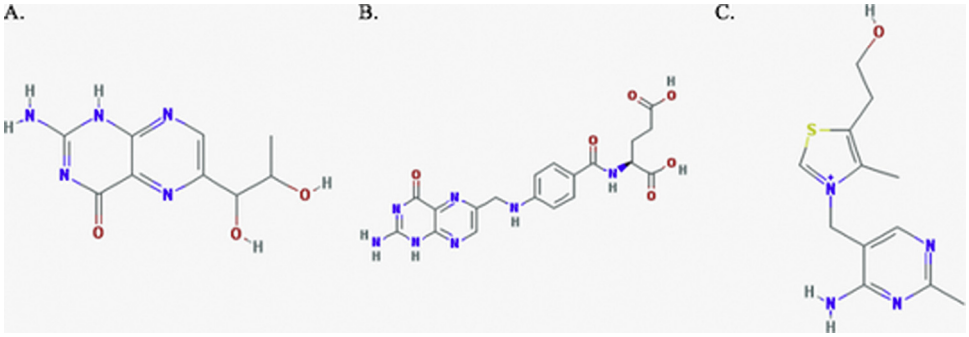

Fig. 3. Chemical structures of (A) biopterin, (B) folate, and (C) thiamine. All images were obtained from the PubChem open chemistry database (https://pubchem.ncbi.nlm.nih.gov). Accession numbers: (A) biopterin, CID 2380; (B) folate, CID6037; (C) thiamine, CID1130.

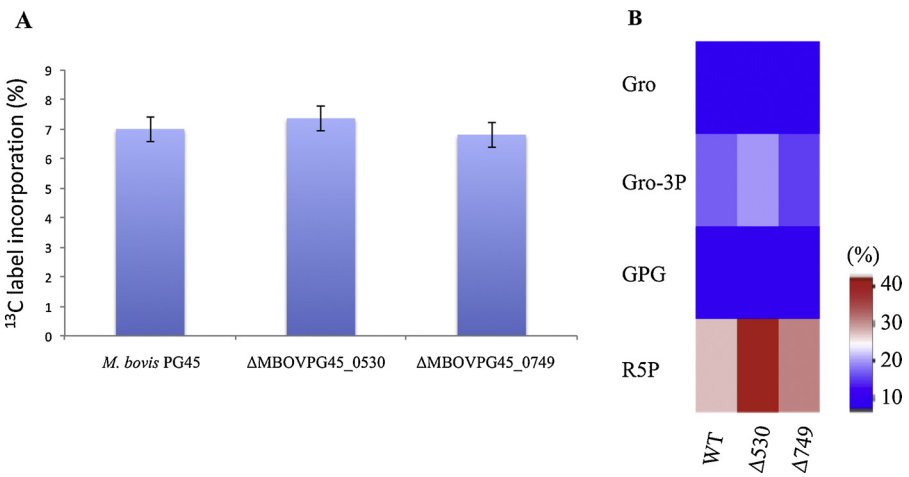

Fig. 4. A. Incorporation of ^{13}C-label into the intracellular glycerol pool (measured by GC/MS) in *M. bovis* PG45, ΔMBOVPG45_0530 and ΔMBOVPG45_0749. Error bars indicate the standard error of the mean from four biological replicates. **B.** Metabolites labelled in *M. bovis* PG45 (WT), ΔMBOVPG45_0530 (Δ530) and ΔMBOVPG45_0749 (Δ749) after culture with ^{13}C-glycerol. The colour scale indicates the proportion of the metabolite containing the label (%). Abbreviations: Gro, glycerol; Gro-3 P, glycerol 3-phosphate; GPG, glycerophosphoryl glycerol.

nucleotide sugars.

Although the operon containing MBOVPG45_0116 (Fig. 1B) contains proteins that have significant similarity to only oligopeptide/dipeptide binding domains, no consistent differences in dipeptides or amino acids were detected between the wild type and ΔMBOVPG45_0116. This suggests that *M. bovis* may have a capacity to compensate for the loss of this transporter, as we observed in our previous study examining amino acid transporters of *Mycoplasma gallisepticum* (Masukagami et al., 2018). Oligopeptide and amino acid uptake are considered to be especially important for growth of *M. bovis*, as their preferential nutrient source has been proposed to be amino or organic acids (Khan et al., 2005; Pollack, 2002), and genome annotation suggests *M. bovis* possesses a predicted oligopeptide transporter (OppABCDF, MBOVPG45_0033, 0034, 0035, 0036, and 0037) that might compensate for loss of function of MBOVPG45_0116. Alternatively, the substrate of the MBOVPG45_0116 transporter may differ from the bioinformatic predictions. The organic acid maleic acid was consistently elevated in the wild type, so further specific experiments investigating substrate specificity are needed.

MBOVPG45_0533 appears to be involved in the uptake of UDP-sugars (UDP-D-galactose and UDP-glucose), as these metabolites were more abundant in the wild type metabolome, and bioinformatic analyses using Phyre^2 (Kelley et al., 2015) support this notion. Although this gene is currently annotated as either a member of the LAT transporter family (BioCyc database (Caspi et al., 2016; Karp et al., 2005; Toya et al., 2011) or as an amino acid transporter (NCBI databases), Phyre^2 analyses showed that the level of confidence and identity of the putative protein to these families is similar to those it has with a nucleobase-cation symporter and a sodium/glucose co-transporter. Amino acid sequence is not a good indicator of substrate specificity for nucleotide sugar transporters (Hadley et al., 2014) and the metabolite profiling strongly suggested that UDP-sugars are a substrate for this transporter. To confirm whether MBOVPG45_0533 is involved in UDP-sugar uptake, further targeted metabolomic experiments, in which MB medium is analysed by LC/MS for UDP-sugar levels during mycoplasma growth, are required. Maleic acid was also consistently elevated in the wild type compared to the MBOVPG45_0533 mutant, and similar targeted experiments would be useful to examine whether it is a substrate for this transporter.

Although MBOVPG45_0568 is annotated as belonging to the DAACS transporter family, the metabolite profiling results did not strongly suggest particular amino acids were the substrate of this transporter. It is possible that compensation by other transporters masked the effects of the mutation. Interestingly, biopterin was significantly and consistently elevated in the wild type and had the highest fold difference. Biopterin is a pteridine compound, as is folate, which contains the biopterin structure (Fig. 3). Biopterin is a component of tetrahydrobiopterin (H4-biopterin), which is an essential cofactor of enzymes in central metabolism, such as the hydroxylases of aromatic amino acids, lipid oxidase and nitric oxide synthase (NOS) isoenzymes in mammals (Werner-Felmayer et al., 2002). The involvement of H4-biopterin in NOS synthesis as virulence factor has been reported in *Norcardia* species and *Mycobacterium* species (Jung et al., 2013; Son and Rosazza, 2000). However, a biopterin biosynthesis pathway has not been detected in mycoplasma species, suggesting that they scavenge biopterin from their environment (Cunningham and Beverley, 2001; Werner-Felmayer et al., 2002). Although some mycoplasma species, such as *Mycoplasma capricolum,* possess a folate transporter (FolT), which is classified in the folate/biopterin transport (FBT) family, no homologues of this transporter are identifiable in *M. bovis* using a BLASTP search. Analysis of the MBOVPG45_0568 amino acid sequence for the seven conserved residues suggested to be critical for FBT function (Eudes et al., 2010) showed that none of them were present. However, Phyre^2 analysis predicted that residues 15–135 of the MBOVPG45_0568 amino acid sequence had a similar protein structure to the S-component of the thiamine transporter ThiT. In humans, folate and thiamine transporters evolved from the same family (Zhao and Goldman, 2013). Further specific experiments examining whether MBOVPG45_0568 transports biopterin are warranted.

The failure to observe differences in glycerol uptake between the wild type and the putative glycerol transporter mutants ΔMBOVPG45_0530 and ΔMBOVPG45_0749 supports the hypothesis that these two different transporter types most probably compensate for each other in their function in uptake of glycerol, and may explain why they are non-essential genes (Sharma et al., 2014). Interestingly, reduced ^{13}C-labelling in the intracellular glycerol pool compared to the Gro-3 P pool was observed in both wild type *M. bovis* PG45 and the mutants. This implies that an alternative route to supply non-labelled glycerol into the intracellular glycerol pool could be active in *M. bovis*. The most likely explanation for this is the existence of a putative transport system related to the membrane lipase, which breaks down triglycerides (present in porcine serum in the MB medium) and supplies glycerol into the intracellular glycerol pool, although no lipase-related transport system has yet been identified in *M. bovis*.

Although MBOVPG45_0307 is annotated as part of a glycerol transporter, Gro-3P and Gro-2P were actually more abundant in ΔMBOVPG45_0307. While it is possible that the product of MBOVPG45_0307 may have an alternative function, it may be that other glycerol transporters, such as the two others studied here (MBOVPG45_0530 and MBOVPG45_0749), compensate for the loss of function in this mutant. This, combined with the lack of significant differences in glycerol uptake between wild type *M. bovis* and the MBOVPG45_0530 and MBOVPG45_0749 mutants, suggest that comparing gene expression levels of the alternative transporters in these *M.*

bovis mutant strains (ΔMBOVPG45_0307, ΔMBOVPG45_0530 and ΔMBOVPG45_0749) to those seen in the wild type has the potential to elucidate compensatory pathways.

In this study, unexpected functions for two different putative amino acid transporters were suggested by metabolomic profiling. This further demonstrates the value of metabolomic analysis in investigating the function of proteins where similarities to other protein families are low or absent. The apparent redundancy observed in some transport systems is also of note in an organism with a reduced genome, emphasising the crucial role of nutrient uptake for the mycoplasma. Studies such as these provide valuable information for future specific studies, such as binding assays using recombinant proteins or transport assays using labelled compounds.

Appendix A. Supplementary data

Supplementary material related to this article can be found, in the online version, at doi:https://doi.org/10.1016/j.vetmic.2019.05.008.

References

Altschul, S.F., Gish, W., Miller, W., Myers, E.W., Lipman, D.J., 1990. Basic local alignment search tool. J. Mol. Biol. 215, 403–410.

Altschul, S.F., Madden, T.L., Schaffer, A.A., Zhang, J., Zhang, Z., Miller, W., Lipman, D.J., 1997. Gapped BLAST and PSI-BLAST: a new generation of protein database search programs. Nucleic Acids Res. 25, 3389–3402.

Ayling, R.D., Baker, S.E., Nicholas, R.A., Peek, M.L., Simon, A.J., 2000. Comparison of in vitro activity of danofloxacin, florfenicol, oxytetracycline, spectinomycin and tilmicosin against *Mycoplasma mycoides* subspecies *mycoides* small colony type. Vet. Rec. 146, 243–246.

Bachmann, B.J., 1990. Linkage map of *Escherichia coli* K-12. edition 8. Microbiol. Rev. 54, 130–197.

Berman, H.M., Westbrook, J., Feng, Z., Gilliland, G., Bhat, T.N., Weissig, H., Shindyalov, I.N., Bourne, P.E., 2000. The protein data bank. Nucleic Acids Res. 28, 235–242.

Caspi, R., Billington, R., Ferrer, L., Foerster, H., Fulcher, C.A., Keseler, I.M., Kothari, A., Krummenacker, M., Latendresse, M., Mueller, L.A., Ong, Q., Paley, S., Subhraveti, P., Weaver, D.S., Karp, P.D., 2016. The MetaCyc database of metabolic pathways and enzymes and the BioCyc collection of pathway/genome databases. Nucleic Acids Res. 44, D471–480.

Caswell, J.L., Archambault, M., 2007. *Mycoplasma bovis* pneumonia in cattle. Anim. Health Res. Rev. / Conf. Res. Workers Anim. Diseases 8, 161–186.

Caswell, J.L., Bateman, K.G., Cai, H.Y., Castillo-Alcala, F., 2010. *Mycoplasma bovis* in respiratory disease of feedlot cattle. Vet. Clin. North Am. Food Anim. Pract. 26, 365–379.

Cunningham, M.L., Beverley, S.M., 2001. Pteridine salvage throughout the *Leishmania* infectious cycle: implications for antifolate chemotherapy. Mol. Biochem. Parasitol. 113, 199–213.

Davidson, A.L., Chen, J., 2004. ATP-binding cassette transporters in bacteria. Annu. Rev. Biochem. 73, 241–268.

Erkens, G.B., Berntsson, R.P., Fulyani, F., Majsnerowska, M., Vujicic-Zagar, A., Ter Beek, J., Poolman, B., Slotboom, D.J., 2011. The structural basis of modularity in ECF-type ABC transporters. Nat. Struct. Mol. Biol. 18, 755–760.

Eudes, A., Kunji, E.R., Noiriel, A., Klaus, S.M., Vickers, T.J., Beverley, S.M., Gregory 3rd, J.F., Hanson, A.D., 2010. Identification of transport-critical residues in a folate transporter from the folate-biopterin transporter (FBT) family. J. Biol. Chem. 285, 2867–2875.

Faham, S., Watanabe, A., Besserer, G.M., Cascio, D., Specht, A., Hirayama, B.A., Wright, E.M., Abramson, J., 2008. The crystal structure of a sodium galactose transporter reveals mechanistic insights into Na+/sugar symport. Science 321, 810–814.

Fox, N.K., Brenner, S.E., Chandonia, J.M., 2014. SCOPe: structural Classification of Proteins–extended, integrating SCOP and ASTRAL data and classification of new structures. Nucleic Acids Res. 42, D304–309.

Fraser, C.M., Gocayne, J.D., White, O., Adams, M.D., Clayton, R.A., Fleischmann, R.D., Bult, C.J., Kerlavage, A.R., Sutton, G., Kelley, J.M., Fritchman, R.D., Weidman, J.F., Small, K.V., Sandusky, M., Fuhrmann, J., Nguyen, D., Utterback, T.R., Saudek, D.M., Phillips, C.A., Merrick, J.M., Tomb, J.F., Dougherty, B.A., Bott, K.F., Hu, P.C., Lucier, T.S., Peterson, S.N., Smith, H.O., Hutchison 3rd, C.A., Venter, J.C., 1995. The minimal gene complement of *Mycoplasma genitalium*. Science 270, 397–404.

Hadley, B., Maggioni, A., Ashikov, A., Day, C.J., Haselhorst, T., Tiralongo, J., 2014. Structure and function of nucleotide sugar transporters: current progress. Comput. Struct. Biotechnol. J. 10, 23–32.

Halbedel, S., Stulke, J., 2007. Tools for the genetic analysis of Mycoplasma. Int. J. Med. Microbiol.: IJMM 297, 37–44.

Jung, J.Y., Madan-Lala, R., Georgieva, M., Rengarajan, J., Sohaskey, C.D., Bange, F.C., Robinson, C.M., 2013. The intracellular environment of human macrophages that produce nitric oxide promotes growth of mycobacteria. Infect. Immun. 81, 3198–3209.

Karp, P.D., Ouzounis, C.A., Moore-Kochlacs, C., Goldovsky, L., Kaipa, P., Ahren, D., Tsoka, S., Darzentas, N., Kunin, V., Lopez-Bigas, N., 2005. Expansion of the BioCyc collection of pathway/genome databases to 160 genomes. Nucleic Acids Res. 33, 6083–6089.

Kelley, L.A., Mezulis, S., Yates, C.M., Wass, M.N., Sternberg, M.J., 2015. The Phyre2 web portal for protein modeling, prediction and analysis. Nat. Protoc. 10, 845–858.

Khan, L.A., Loria, G.R., Ramirez, A.S., Nicholas, R.A., Miles, R.J., Fielder, M.D., 2005. Biochemical characterisation of some non fermenting, non arginine hydrolysing mycoplasmas of ruminants. Vet. Microbiol. 109, 129–134.

Kowalski, G.M., De Souza, D.P., Burch, M.L., Hamley, S., Kloehn, J., Selathurai, A., Tull, D., O'Callaghan, S., McConville, M.J., Bruce, C.R., 2015. Application of dynamic metabolomics to examine *in vivo* skeletal muscle glucose metabolism in the chronically high-fat fed mouse. Biochem. Biophys. Res. Commun. 462, 27–32.

Laguri, C., Phillips-Jones, M.K., Williamson, M.P., 2003. Solution structure and DNA binding of the effector domain from the global regulator PrrA (RegA) from *Rhodobacter sphaeroides*: insights into DNA binding specificity. Nucleic Acids Res. 31, 6778–6787.

Lee, N., 2009. Characterization of an ATP-binding Cassette (ABC) Transport System Involved in Nucleoside Uptake in Mycoplasma bovis Strain M23, and Discovery of Its Pathogenicity Genes. Graduate Theses and Dissertations. Iowa State University, Ames, Iowa.

Masukagami, Y., Tivendale, K.A., Mardani, K., Ben-Barak, I., Markham, P.F., Browning, G.F., 2013. The *Mycoplasma gallisepticum* virulence factor lipoprotein MslA is a novel polynucleotide binding protein. Infect. Immun. 81, 3220–3226.

Masukagami, Y., Nijagal, B., Tseng, C.W., Dayalan, S., Tivendale, K.A., Markham, P.F., Browning, G.F., Sansom, F.M., 2018. Metabolite profiling of *Mycoplasma gallisepticum* mutants, combined with bioinformatic analysis, can reveal the likely functions of virulence-associated genes. Vet. Microbiol. 223, 160–167.

Minion, F.C., 2002. Molecular pathogenesis of mycoplasma animal respiratory pathogens. Front. Biosci.: J. Virtual Library 7, 1410–1422.

Nicholas, R.A., Ayling, R.D., 2003. *Mycoplasma bovis*: disease, diagnosis, and control. Res. Vet. Sci. 74, 105–112.

Nicholas, R., Ayling, R., McAuliffe, L., 2007. Mycoplasma mastitis. Vet. Rec. 160 (382), 383 author reply.

Pfutzner, H., Sachse, K., 1996. *Mycoplasma bovis* as an agent of mastitis, pneumonia, arthritis and genital disorders in cattle. Rev Sci. Tech. 15, 1477–1494.

Pollack, J.D., 2002. Central carbohydrate pathways: metabolic flexibility and the extra role of some "housekeeping" enzymes. Molecular Biology and Pathogenicity of Mycoplasmas. Springer Science + Business Media, New York, pp. 163–199.

Razin, S., 1969. Structure and function in mycoplasma. Annu. Rev. Microbiol. 23, 317–356.

Razin, S., Yogev, D., Naot, Y., 1998. Molecular biology and pathogenicity of mycoplasmas. Microbiol. Mol. Bio. Rev.: MMBR 62, 1094–1156.

Rodriguez, F., Bryson, D.G., Ball, H.J., Forster, F., 1996. Pathological and immunohistochemical studies of natural and experimental *Mycoplasma bovis* pneumonia in calves. J. Comp. Pathol. 115, 151–162.

Rosengarten, R., Citti, C., 1999. The role of ruminant mycoplasmas in systemic infection. In: Stipkovits, L., Rosengarten, R., Frey, J. (Eds.), Mycoplasmas of Ruminants: Pathogenicity, Diagnostics, Epidemiology and Molecular Genetics. European Commision, Brussells, pp. 14–17.

Roy, A., Kucukural, A., Zhang, Y., 2010. I-TASSER: a unified platform for automated protein structure and function prediction. Nat. Protoc. 5, 725–738.

Saier Jr., M.H., 2000. A functional-phylogenetic classification system for transmembrane solute transporters. Microbiol. Mol. Biol. Rev. MMBR 64, 354–411.

Saunders, E.C., Ng, W.W., Kloehn, J., Chambers, J.M., Ng, M., McConville, M.J., 2014. Induction of a stringent metabolic response in intracellular stages of *Leishmania mexicana* leads to increased dependence on mitochondrial metabolism. PLoS Pathog. 10, e1003888.

Sharma, S., Markham, P.F., Browning, G.F., 2014. Genes found essential in other mycoplasmas are dispensable in Mycoplasma bovis. PLoS One 9, e97100.

Son, J.K., Rosazza, J.P., 2000. Cyclic guanosine-3',5'-monophosphate and biopteridine biosynthesis in *Nocardia* sp. J. Bacteriol. 182, 3644–3648.

Stemke, G.W., Robertson, J.A., 1982. Comparison of two methods for enumeration of mycoplasmas. J. Clin. Microbiol. 16, 959–961.

Sumner, L.W., Amberg, A., Barrett, D., Beale, M.H., Beger, R., Daykin, C.A., Fan, T.W., Fiehn, O., Goodacre, R., Griffin, J.L., Hankemeier, T., Hardy, N., Harnly, J., Higashi, R., Kopka, J., Lane, A.N., Lindon, J.C., Marriott, P., Nicholls, A.W., Reily, M.D., Thaden, J.J., Viant, M.R., 2007. Proposed minimum reporting standards for chemical analysis Chemical Analysis Working Group (CAWG) Metabolomics Standards Initiative (MSI). Metabolomics 3, 211–221.

Toya, Y., Kono, N., Arakawa, K., Tomita, M., 2011. Metabolic flux analysis and visualization. J. Proteome Res. 10, 3313–3323.

Tozzi, M.G., Camici, M., Mascia, L., Sgarrella, F., Ipata, P.L., 2006. Pentose phosphates in nucleoside interconversion and catabolism. FEBS J. 273, 1089–1101.

Truniger, V., Boos, W., 1993. Glycerol uptake in *Escherichia coli* is sensitive to membrane lipid composition. Res. Microbiol. 144, 565–574.

Voelker, L.L., Dybvig, K., 1996. Gene transfer in *Mycoplasma arthritidis*: transformation, conjugal transfer of Tn*916*, and evidence for a restriction system recognizing AGCT. J. Bacteriol. 178, 6078–6081.

Werner-Felmayer, G., Golderer, G., Werner, E.R., 2002. Tetrahydrobiopterin biosynthesis, utilization and pharmacological effects. Curr. Drug Metab. 3, 159–173.

Weyand, S., Shimamura, T., Yajima, S., Suzuki, S., Mirza, O., Krusong, K., Carpenter, E.P., Rutherford, N.G., Hadden, J.M., O'Reilly, J., Ma, P., Saidijam, M., Patching, S.G., Hope, R.J., Norbertczak, H.T., Roach, P.C., Iwata, S., Henderson, P.J., Cameron, A.D., 2008. Structure and molecular mechanism of a nucleobase-cation-symport-1 family transporter. Science 322, 709–713.

Wise, K.S., Calcutt, M.J., Foecking, M.F., Roske, K., Madupu, R., Methe, B.A., 2011. Complete genome sequence of *Mycoplasma bovis* type strain PG45 (ATCC 25523). Infect. Immun. 79, 982–983.

Zhao, R., Goldman, I.D., 2013. Folate and thiamine transporters mediated by facilitative carriers (SLC19A1-3 and SLC46A1) and folate receptors. Mol. Aspects Med. 34, 373–385.